

The nature of solar flares associated with coronal mass ejection

R.A. Harrison

Astrophysics Division, Rutherford Appleton Laboratory, Chilton, Didcot, Oxfordshire OX11 0QX, UK

Received 27 August 1993 / Accepted 20 May 1995

Abstract. An analysis is presented of solar X-ray flares associated with coronal mass ejections through the period 1986–1987. The nature of the flares apparently associated with mass ejection is explored. In particular the relationships between flare duration and intensity and the association with mass ejection are investigated. We believe that this study tackles the flare-CME analysis in a way that is uniquely unbiased. Past studies of a similar nature are discussed and a criticism of their approach is given. In particular, the author believes that the continual bias toward the so-called Long Duration Events and the brightest flares is misleading. The analysis supports the view that the flare and CME are signatures of the same magnetic “disease”, that is, they represent the responses in different parts of the magnetic structure, to a particular activity; they do not drive one another but are closely related. The present statistical analysis allows a chance association to be given for a mass ejection event when an X-ray flare is observed. The use of such information in the prediction of geomagnetic activity generated when mass ejecta interact with the Earth is discussed.

Key words: Sun: corona – Sun: flares – Sun: magnetic fields – Sun: solar-terrestrial relations

1. Introduction

A coronal mass ejection (CME) involves a significant restructuring of the solar corona as a large-scale eruption carries up to 10^{13} kg of material into interplanetary space. The nature and evolution of such eruptions has been the subject of many reviews, notably, in recent years, Hundhausen (1988, 1993a), Harrison (1991), Kahler (1992) and Dryer (1994). The study of the onset or launch of CMEs has been the subject of much debate since their discovery a little over 20 years ago.

CME activity has been associated with active features on the Sun, such as prominences and flares, and is a clear source of interplanetary clouds. Thus, an understanding of the processes involved in the launch of CMEs is not only of interest for the study of coronal structure and evolution, but has relevance also for the study of other solar active features, the nature of the heliosphere and also for the prediction of geomagnetic activity, generated when ejecta interact with the Earth.

In the corona, a CME is detected by observing photospheric light which is Thomson scattered off free electrons which are concentrated in the magnetic features of the CME. Due to the relative brightness of the solar disc itself, which is some six orders of magnitude brighter than the coronal features, one must obscure the disc to monitor the corona in order to look for CME activity. Further, due to the level of scattered light in the Earth’s atmosphere, most coronal observations of this kind are made using coronagraphs from orbiting spacecraft.

Two features of this observing technique have served to complicate our investigations of CME onsets. First, due to the Thomson scattering process, a CME is best observed in the plane of the sky. Events out of the plane of the sky suffer a significant drop in intensity with increasing angle from the solar limb (e.g. Fisher & Munro 1984; Hundhausen 1993b). Thus, the best observed events have sources which are on or near the solar limb and we must contend with severe foreshortening and the fact that many features associated with the CME onset may be obscured by the Sun’s limb. Second, since we must occult the Sun’s disc, which necessarily results in obscuration of the lowest portions of the corona as well, some back-projections are necessary, in space and time, to investigate the onset location and time.

Several workers have presented careful analyses of individual CME events which have clearly linked coronal and, for example, chromospheric activity at the time of CME onsets, and these must put boundaries on the range of possible CME onset models. As far back as 1979, it was realised that there was an association between flare activity and mass ejections (Munro et al. 1979). However, the association has turned out to be so complex that, to this day, the exact relationship is still hotly debated.

Many studies of the CME-flare relationship have been made. These include the CME-X-ray flare studies due to Sheeley et al. (1983), Harrison (1986), Harrison & Sime (1989, 1992), Kahler et al. (1989), Harrison et al. (1990), St Cyr & Webb (1991) and Hundhausen (1993a). It has become clear that there is a very significant association between the flare process and the CME onset. This must provide clear requirements for any CME-onset model, or, indeed, any flare model. However, models which encompass both phenomena are rare. This is primarily because the precise relationship between the CME and flare is not at all clear.

Let us attempt to summarise, briefly, the salient features of earlier CME-X-ray flare studies:

1. There is an association between CME onsets and flare activity,
2. Flares and CMEs do not appear to occur on a one to one basis,
3. For apparently associated events, the relative timing of the flare-onset and the CME-onset is variable – the onsets can be co-incident or either onset can lead the other by up to many tens of minutes,
4. The characteristics of CME-associated flares (brightness, duration, size etc...) appear to have no relationship to the characteristics of the associated CME (velocity, size etc...),
5. The relative location of a CME and an associated flare is variable – the flare can be anywhere in the vicinity of the CME,
6. The CME generally originates from a much larger source structure than the flare.

In addition, there is a further association which has been published but requires clarification and, indeed, confirmation. This is the apparent association between CME onsets and flare soft X-ray precursors reported for some data-sets (Simnett & Harrison 1985; Harrison et al. 1985).

So, what do we require now in order to progress in the modelling of CME-onsets and associated activity? It is the author's opinion that progress is positively hindered by unfortunate bias in many published analyses. For example, despite clear demonstrations of CME events which cannot be the coronal response to flare-blasts (e.g. Harrison 1986; Hundhausen 1993a), there is still a belief within portions of the solar physics community that this can be the case (see discussion in Harrison & Sime 1989). On another front, specific flare-types are often selected for studies of CME associations, such as bright flares (e.g. Kahler et al. 1989) or the so-called Long Duration Events (e.g. Sheeley et al. 1975; Kahler et al. 1977; Webb & Hundhausen 1987). This is particularly true for almost all CME-flare statistical studies. Such selection can often mask the true relationship of two phenomena.

It is time, in the author's opinion, that a clear, unbiased statistical study was performed, in order to strengthen our understanding of the CME-flare relationship. Such a study may bring out the same results as earlier statistical work, but at least a clear demonstration will have been made. This is the purpose of this work. Thus, in this study we present a statistical analysis of CME and flare activity for the years 1986 and 1987, and take steps to ensure that no bias is introduced through event selection. We choose the 1986–7 period, which is near to solar minimum, to minimize chance associations. In addition to the statistical report, we discuss the results of past studies, highlight any failings of these studies and discuss their findings in relation to those of the present work.

2. The data

For the CME data, we make use of the Solar Maximum Mission (SMM) Coronagraph data-set (courtesy of A.J. Hundhausen,

High Altitude Observatory). These data are summarized in Burkepile & St Cyr (1993). We listed 151 CMEs for the 2 year period and for each event, noted the year of observation, the time of first observation, the projected onset (assuming a zero altitude onset, on the limb, with no acceleration), the centre of the CME (position angle – given anti-clockwise from solar north), the CME span and the outward propagating velocity of the CME. We reject CMEs with measured speeds of ascent slower than 50 km s^{-1} in recognition of the difficulties in identifying the onset times of such events (see later). All data used are taken from Burkepile & St Cyr (1993) except for the projected onset time which was supplied by A.J. Hundhausen (private communication).

For the flare data, we use 1–8 Å X-ray observations from the GOES satellite series and $\text{H}\alpha$ information from ground based observatories. The latter are listed in *Solar Geophysical Data* (SGD; US Dept of Commerce) and are only used in this study to obtain information on flare locations. The GOES profiles are for integrated-Sun. The profiles and event lists, taken from the profiles, are given in SGD.

In order to associate the flare and CME events we require the time of flare onset and the flare location. To study the properties of the CME-associated flares, we require also the duration and the maximum X-ray flux. The SGD event lists can be misleading since events are often defined by the crossing of thresholds rather than absolute changes, and listed intensities are given without background subtraction. For this reason we have examined the entire 1986–7 GOES X-ray profile and produced our own event list. Of course, the identification of an event is somewhat subjective; one has to use selection criteria which are unlikely to influence the results of the study being performed. For example, the selection of flares which exceed a specified intensity or duration could place a clear bias on the results. A flare is, of course, characterised by a brightening in X-rays, so one would define the onset as the time that the X-ray profile first assumes a positive slope and the peak intensity as the maximum intensity achieved minus the pre-flare background intensity. Specifically, we have chosen the following selection criteria, and stress that they do not influence the results of our study:

- (a) An event is identified if the X-ray intensity curve shows a positive slope, equivalent to a half decade increase in intensity per hour (in $\text{W}^{-2} \text{ hr}^{-1}$), for more than 5 minutes.
- (b) The flare onset time is the time of the first clear positive increase of this slope.
- (c) The peak flux is noted and the approximate background level prior to the event is subtracted.
- (d) The definition of the end time, required for the duration calculation, is more tricky due to event superposition, to background level changes etc... Thus, we define the end of the event as the point where the intensity falls to within 20% of the pre-event intensity, or the X-ray profile has become flat over an extended period of time.

In the analysis, we define the flare rise-time as the time between the flare onset and peak times, as defined above, and

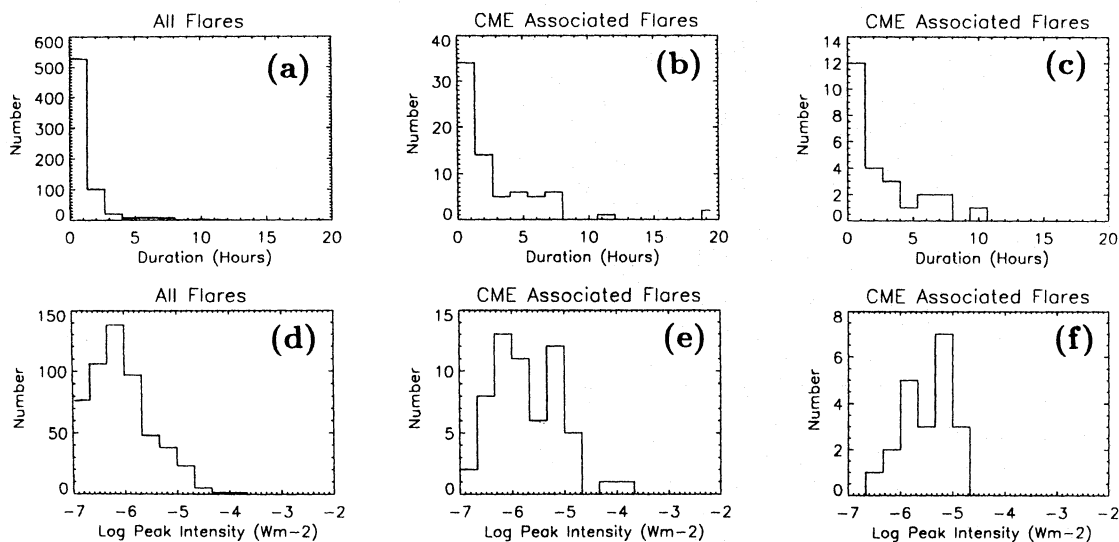


Fig. 1a–f. The distribution of flare durations for **a** the 674 X-ray flares in the study, **b** the 72 X-ray flares which fall within the CME onset windows for the temporal analysis, and **c** the 25 X-ray flares which fall within the CME onset windows for the temporal and spatial analysis. The distribution of peak intensities for **d** the 674 X-ray flares in the study, **e** the 72 X-ray flares which fall within the CME onset windows for the temporal analysis, and **f** the 25 X-ray flares which fall within the CME onset windows for the temporal and spatial analysis

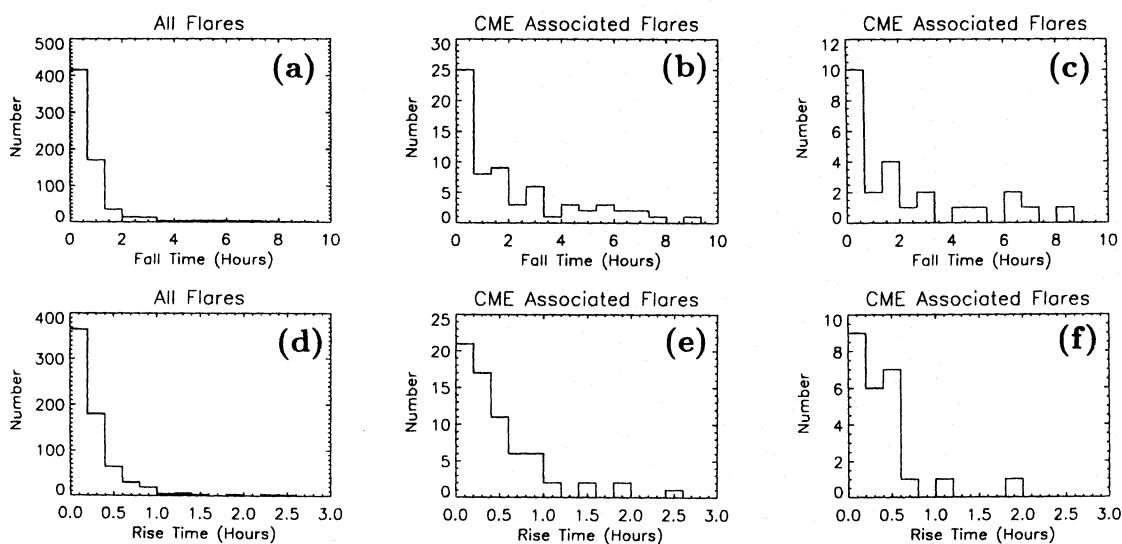


Fig. 2a–f. The distribution of fall times for **a** the 674 X-ray flares in the study, **b** the 72 X-ray flares which fall within the CME onset windows for the temporal analysis, and **c** the 25 X-ray flares which fall within the CME onset windows for the temporal and spatial analysis. The distribution of rise times for **d** the 674 X-ray flares in the study, **e** the 72 X-ray flares which fall within the CME onset windows for the temporal analysis, and **f** the 25 X-ray flares which fall within the CME onset windows for the temporal and spatial analysis

the flare fall-time is the time between the peak and the event end time as defined above.

The first of the selection criteria was used to identify 674 X-ray flares for the 1986–7 period. The distribution of durations and intensities for these are given in Figs. 1a and 1d, and the distributions of the rise and fall times are shown in Figs. 2a and 2d.

3. A temporal analysis

Let us examine first the data-sets purely on the basis of a temporal association. The logical approach is to define a time window

which includes the onset of the CME and look for associated flare activity within that window. One could define the window as being centred on the projected onset time of the CME. However, the projection assumes (i) zero acceleration below the coronagraph occulting disc, (ii) a zero altitude onset, and (iii) a source structure located at the limb. We know that CMEs often experience acceleration. Thus, for the slower CMEs the onset window may be located some time after the actual onset of the CME – but we have countered this by only including CMEs with velocities of ascent above 50 km s^{-1} . However, for CMEs which are well out of the plane of the sky, the actual onset may be prior to the projected onset as the source region is well onto

the disc. This is a relatively small effect. For example, for a CME source region some 30° out of the plane of the sky, this would produce a projected onset some 7, 3.5, 2 and 1.6 minutes earlier than the limb-projected onset, for speeds of 100, 200, 350 and 450 km s^{-1} , respectively. The average CME velocity of ascent is about 350 km s^{-1} . Finally, the source structures most likely extend well into the corona so the projected onset should not go to a zero altitude, making our projected onsets earlier than the actual onsets.

Another approach is to accept that (i) since we have eliminated the slowest CMEs, (ii) since the out of the plane of the sky effect is relatively small, and (iii) since the source structures undoubtedly have some initial altitude which is probably quite large, we should open an onset window centred on the point of first observation of the CME. This will, of course be above 1.5 solar radii from Sun centre for this study. To assess the value of such a scheme, we note that if the CME did in fact start from zero altitude and if the first observation was made at 1.5 solar radii, the offset of the window centre from the CME onset would be 58, 29 and 17 minutes for speeds of 100, 200 and 350 km s^{-1} , respectively. In view of the fact that we will be opening windows of duration several hours, it seems perfectly reasonable to centre the window on the time of the first CME observation.

From previous studies, it is clear that a window of size $\pm N$ hours on either side of the first CME observation, where N is of order a few hours or less, is quite reasonable. However, there is little evidence to suggest precisely what value of N one should choose. So, for this temporal study, we choose $N = 2$. At a time of solar minimum, i.e. the period of this study, the definition of such a window should have very little influence on the final results. However, it is clear that larger windows will introduce more chance associations and smaller windows may omit real associations.

In opening a ± 2 hour ‘‘onset’’ window on either side of the time of first observation of each CME we find that in the period from 1 January 1986 to 31 December 1987, during which 674 X-ray flares and 151 CMEs were detected, some 72 flares fall within the CME onset windows. Due to some co-incidence associations, i.e. some windows contain two flares, this reduces to 61 CMEs with a flare in the onset window, as defined.

Given a random situation, over a 2 year period, with the same number of CMEs and flares, one would expect to find $(151 \text{ CMEs} \times 4 \text{ hours} \times 674 \text{ flares} / 365 \text{ days} \times 2 \text{ years} \times 24 \text{ hours}) = 23.2$ flare events in the CME onset windows, i.e. we see a factor of 3.1 more events than expected. This suggests a very high degree of association between the flare events and the CME onsets.

Suppose that for every CME there is a flare and vice versa. Let us assume that the 674 flares are distributed evenly over the visible disc of the Sun and that there is the same number of flares on the far side of the Sun. Assuming that CMEs can only be observed within $\pm 40^\circ$ of the limbs, we may expect to see 599 CMEs, and would expect to see associations with 300 flares of the 674. We see, in fact, 155 CMEs, with apparent associations with 72 flares. There may be significant sensitivity

effects, i.e. CME or X-ray flare events which are not detected by current instrumentation, as well as problems in defining and identifying flares and CMEs, but thus far in this study we must state that many flares do not appear to have an association with an observed CME.

The ± 2 hour window ensures that events associated with CME onsets for CME speeds down to about 49 km s^{-1} are covered. This assumes that the onset is from a zero altitude, that there is no net acceleration/deceleration prior to the first observation, and that the first observation is made at an altitude of $0.5 R_\odot$. Given that CME speeds are commonly a few hundred km s^{-1} , though they are observed in the range a few tens of km s^{-1} to $\sim 2000 \text{ km s}^{-1}$, and that the majority of CMEs are observed to emerge from behind the occulting disc of the SMM coronagraph, the onsets for the majority of CMEs would be contained within the windows as defined. Thus, the statistical associations given above can be trusted.

So, what is special, if anything, about the flares which appear to be associated with the CME onsets?

The average duration of the 674 flare events is 1.14 hours. This compares to an average of 3.01 hours for the 72 flares found in the CME onset windows – a factor of 2.6 longer. The precise distributions of durations are shown in Figs. 1a and 1b. Both show a Poisson-like curve with similar peaks at the shortest durations and a fall-off toward greater durations. These are suggestive of single-event type distributions; we do not see structure in the curves due to different classes of flare, such as long duration events. The only clear difference between the two curves is that the CME-associated curve falls off much more slowly. Despite the low numbers, this enhanced tail is significant in comparison to the full X-ray flare data-set.

These results show that a CME can be associated with an X-ray flare of *any* duration. Indeed, 61% of the CME-associated flares have durations of less than 2 hours. However, a longer duration flare has a greater chance of having an associated CME. If we simply divide the numbers given in Figs. 1a and 1b, there appears to be a 6.4% chance of a flare of duration about 1 hour having an observed CME association, whereas there appears to be a 50% chance of a flare of duration 6 hours having an observed CME association.

The peak $1\text{--}8 \text{ \AA}$ flux at 1AU for the full-flare data-set is $2.3 \times 10^{-6} \text{ W m}^{-2}$ whilst the peak flux for the CME-associated flares is $6.3 \times 10^{-6} \text{ W m}^{-2}$, a factor of 2.7 greater. The distributions of peak fluxes are shown in Figs. 1d and 1e. The GOES fluxes are commonly classified in terms of B, C, M and X etc... events, where these represent intensities of 10^{-7} W m^{-2} , 10^{-6} W m^{-2} , 10^{-5} W m^{-2} , 10^{-4} W m^{-2} , respectively. Each decade is split into ten divisions, thus giving classifications such as C1, M3, X5 etc... The full-flare distribution shows a wide spread, peaking at about C1 with a steep fall-off and little above the M1 level. Although the CME-associated flares show a similar spread, indicating that a CME-associated flare can be of any intensity, the structure is different, with two isolated peaks at C1 and M1. These appear to be statistically significant.

The rise times for the full-flare data-set average at 0.27 hours, and the fall-time is 0.87 hours, showing the tradi-

Table 1. Tabulated random and actual flare-CME associations for different flare classes

Flare class	No. in 1986/7	No. expected in CME windows at random	No. actually detected in CME windows (% of total)	Ratio of observed to expected
B	337	11.6	23 (6.8%)	1.98
C	251	8.7	38 (15.1%)	4.37
M	38	1.3	9 (23.7%)	6.92
X	1	0.03	1	?

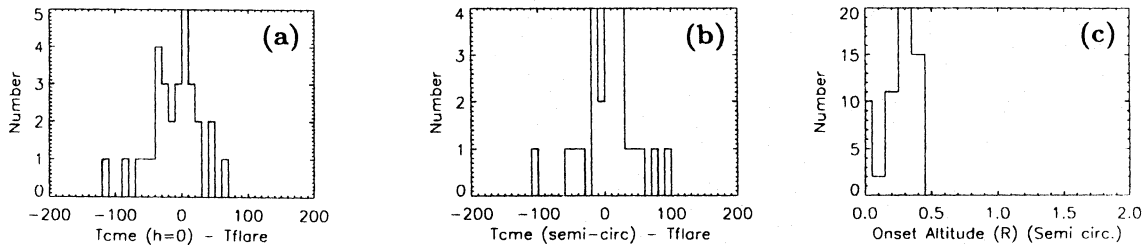


Fig. 3. **a** The relative timing between the projected onset of the CME to the onset of the associated flare, for the events of the temporal analysis which are within the CME onset windows as defined. See text for discussion. **b** A similar display to the first panel assuming a projected CME onset to a semi-circular loop-top, rather than the limb, the loop size being defined by the measured separation of the footpoints of the CME. **c** The distribution of onset altitudes assuming a semi-circular geometry as discussed in the text

tional flare profile of shorter rise than decay. For the CME-related flares, the rise-time average is a factor of 1.8 longer, and, more significantly, the fall-time is a factor of 3.1 longer. Thus, the CME-related flares show significantly longer fall-times in relation to the rise-times, i.e. the profiles are less symmetrical than the full-flare data-set average. The distributions of fall-times and rise-times are shown in Fig. 2, and these clearly show, again, a single-event type distribution with Poisson-like curves in all cases, i.e. a CME-related flare can be associated with any value of fall- and rise-time.

Let us examine the chances for flare CME associations as a function of flare classification. For each class of flare (i.e. B, C, M and X), assume a random situation. Thus, if we detect P flares, for a total window duration of 151×4 hours in 2 years, we would expect $0.034 P$ flares to occur within the windows. For each class, we calculate the expected occurrence and these are compared to the actual occurrence in Table 1.

Based on the numbers in Table 1, we can state that the data suggest the following:

- There is a 6.8% chance of detecting a CME in association with a B-class flare,
- There is a 15.1% chance of detecting a CME in association with a C-class flare,
- There is a 23.7% chance of detecting a CME in association with an M-class flare.

For the X-class events, the 1 event during the period under study was found within a CME-onset window.

Figure 3a shows the relative timing between the projected onset of the CME to the onset of the associated flare, for those events where a flare has been detected in the CME-onset windows as defined. Alas, projected onset times were not available for all of the CMEs, so the plot contains only 30 events. In other

words, of the total set of 151 CMEs, we had 61 with flares in the CME onset windows, as defined, and of those 61 CMEs, only 30 have projected onset times. The projected onset is the apparent onset assuming no acceleration behind the coronagraph occulting disc, with a zero altitude onset on the limb. This is, of course, an extremely rough guide to the onset time since a significant acceleration phase might occur and the altitude of onset may be at a very significant height. Nevertheless it gives a useful view of the situation.

In Fig. 3a, positive values are those where the flare apparently starts prior to the projected CME-onset and negative values are those for which the CME onset apparently leads the flare onset. The units are in minutes. A zero value suggests that the flare and CME onsets are co-incident. In fact, we find a wide peak, of width at half maximum of about 80 minutes, peaking at the 0 to +10 minute bin. Immediate inspection suggests that CME and flare onsets are closely associated but that they may occur anywhere within a few tens of minutes with respect to one another.

If there is significant acceleration during the early stages of the CME, our back-projection is in error and the entire distribution would shift to the left with respect to the axis – the CME-leads-flare scenario would dominate. Given a non-zero altitude onset, the curve would shift to the right – toward the flare-leads-CME scenario.

One quick method for examining this further is to take into account the size of each CME. We know the footpoint separations of the CMEs from the listings and, if we assume a circular geometry, we can simply project the CME to the top of the assumed semi-circular loop rather than to the limb. This gives the distribution of Fig. 3b, with the onset altitudes of Fig. 3c. Such altitudes are consistent with the discussion of Hundhausen (1993a). However, still we have not considered acceleration,

Table 2. A comparison of results for various onset windows

Window duration (hours)	No. of flares in CME windows	Enhancement rel. to random	Ratio of flare durations (CME/all)	Ratio of flare peak intensities (CME/all)
± 1	40	3.4	2.9	3.9
± 2	72	3.1	2.6	2.7
± 3	94	2.7	2.5	2.4

there are 10 events where the CME onset appears to lead the flare *without acceleration being considered* and the distribution still shows a spread of ± 100 minutes. We must conclude that the data support the view that the CME and flare onset are closely associated but that they can occur at any time within several tens of minutes of one another. Thus, the flare in the general case does not drive the CME and vice versa.

Finally, in this analysis, we examine briefly the effects of using different windows, to convince ourselves that the 2 hour window was reasonable. Table 2 shows several of the parameters given in the text above compared to identical analyses with 1 and 3 hour windows. They indicate quite clearly that the 2 hour window can be taken as representative.

4. A temporal and spatial analysis

Now we examine the properties of the same data-set using events for which we can make both temporal and spatial associations. Remember that for the two-year period there were 151 recorded CMEs and 674 X-ray flares. To provide spatial associations we require information on the flare location, which is not available through the GOES X-ray data alone. Thus, for each of the 674 flare events any $H\alpha$ flare co-incidences have been sought. These associations were done by direct comparisons of the X-ray flare list derived as described above, with the $H\alpha$ “grouped” flare listings in SGD. It is believed that of the 674 X-ray flares, for 414 we can make very good $H\alpha$ associations, and thus derive information on location. It should be noted that the X-ray emission from a flare commonly extends well into the corona, whilst the $H\alpha$ emission is basically chromospheric. Thus, for many near-limb flares one may record an X-ray event with no accompanying $H\alpha$ counterpart – we would not expect a 100% association.

This time, let us open a ± 3 hour window on either side of the first observation of a CME. As demonstrated in the last section, such a window is reasonable. Since the counting statistics will be lower in this portion of the study, a slightly larger window may be useful in that it may encompass some more related events which were omitted in the last section. However, varying the window in this manner will not influence the result.

Let us demand that, for an acceptable association, the flare must lie within 50° of the limb, in longitude and that the flare must be within a latitude range defined by a 20° degree margin on either side of the CME-span. We use a longitude of 50° since this is the value at which the CME brightness has fallen by 50%, according to Fisher & Munro (1984). A more recent

study by Hundhausen (1993b) suggests that a more rapid fall-off with angle is more appropriate, perhaps falling to 50% by about $35\text{--}40^\circ$ for an average sized CME. However, since we do not wish to pre-suppose that any CME-associated flare lies under the CME, we will continue with the 50° figure.

Only 188 of the flares lay within 50° of the limb, thus reducing the pool for associated flares still further. We find that 25 of the 188 flares fall within the defined windows of the 151 CMEs. Conversely, some 21 CME windows encompassed one or more flare. Given a random situation, we would have expected $(151 \text{ CMEs} \times 6 \text{ hours} \times 188 \text{ flares} / 365 \text{ days} \times 2 \text{ years} \times 24 \text{ hours} \times 2 \text{ limbs}) = 4.86$ CME associated flares. (The final factor of 2 in the calculation is to cater for the fact that we are covering two limbs and we are assuming an equal chance of flares on the east and western limbs.) This figure is an overestimate since we have made no allowance for the latitude demands for an acceptable association in this random figure. Even so, we find an “expected” association which is a factor of 5.1 less than that which we see. Thus, with the spatial element, as well as the temporal element considered, the association between the flare and the CME-onset described in the last section is enhanced considerably.

So, again, what is special, if anything, about the flares which appear to be associated with the CME onsets in this spatial and temporal analysis?

The average duration of the full list of 674 flares was 1.14 hours. This compares to an average of 2.77 hours for the 25 CME-associated flares in this portion of the study. This is a factor of 2.4 longer. This compares favourably with the results of the last section. The precise distribution of durations for the 25 events is shown in Fig. 1c. As before, the only clear difference between this curve and the curve for the full-flare data-set is that the CME-associated curve falls off much more slowly. Despite the very low numbers, this enhanced tail is significant in comparison to the full X-ray flare data-set. These results confirm the fact that CMEs are associated with the full range of flare durations, but that there is an enhanced association with *longer duration* events.

The peak 1–8 Å flux at 1AU for the full-flare data-set is $2.3 \times 10^{-6} \text{ W m}^{-2}$ whilst the peak flux for the CME-associated flares of the current analysis is $5.1 \times 10^{-6} \text{ W m}^{-2}$, a factor of 2.2 greater. Again, this is in keeping with the results of the last section. The distribution of peak fluxes is shown in Fig. 1f. We are now seeing a clear peak at the M1 level, with a gradual increase with flux to a cut-off to higher fluxes. This is in contrast to the full-flare curve which peaks at much lower fluxes. The tempo-

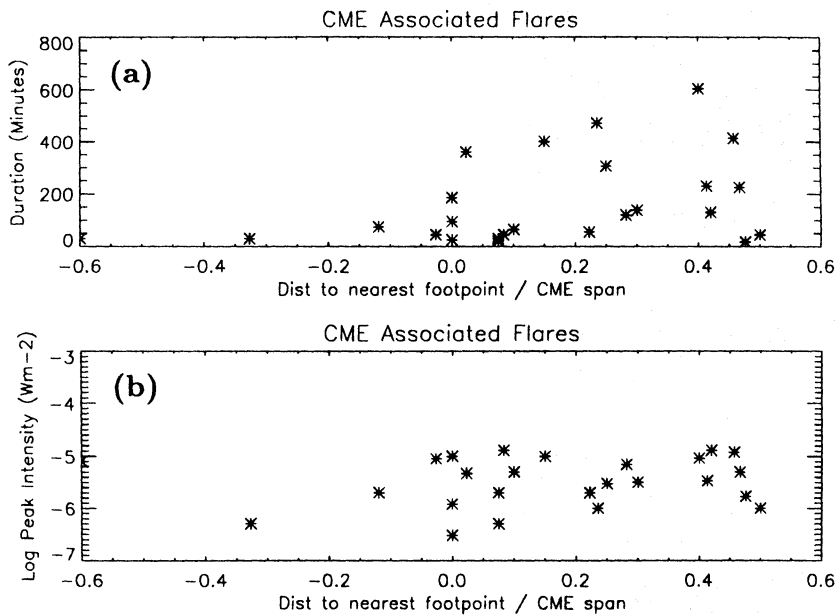


Fig. 4a and b. Plots of the ratio of the distance of the CME-associated flare from the nearest CME footpoint to the CME span versus **a** the CME velocity of ascent and **b** the peak X-ray flux. A value of the ratio of 0.0 represents a situation where a flare lies at the footpoint of its associated CME. A value of 0.5 would be where the flare lies under the core of the CME-span. A negative value is where the flare lies outside the CME-span

ral study showed a hybrid of the two curves (Fig. 1e) suggesting that the spatial information was crucial in highlighting the “real” association for this particular feature.

For the CME-related flares, in this portion of the analysis, the average rise time is a factor of 1.5 longer, and the fall-time is a factor of 2.7 longer than the full-flare data-set. These are consistent with the results of the last section, and it confirms that the CME-related flares show significantly longer fall-times in relation to the rise time, i.e. the profiles are less symmetrical than the full-flare data-set. The distributions of fall-times and rise-times are shown in Fig. 2.

Since we have spatial information, we now discuss the association between the CME-span and the flare location. Figure 4 shows plots of the ratio of the distance of the flare from the nearest CME footpoint to the CME span, versus the (a) flare duration and (b) peak X-ray flux. A value of the ratio of 0.0 is where a flare lies at the footpoint of its associated CME. A value of 0.5 would be where the flare lies under the core of the CME-span. A negative value is where the flare lies outside the CME-span. Data are shown for the 25 events discussed above. Some 84% lie within the CME span; 46% fall in the range 0.0–0.25, and 38% lie in the range 0.25–0.5. Thus, the flare can occur anywhere in the vicinity of the CME-span, but with a preference to be within it – there is no evidence for a preferred site. This is in keeping with the conclusions of recent studies (e.g. Harrison et al 1990; Harrison 1991; Kahler et al. 1989).

Figure 4 also indicates, quite clearly, that there is no relationship between the flare-site, with respect to the CME-span, and the flare parameters of duration and intensity. This could be considered to be a surprising result since a flare situated under the leg of a CME could apparently occupy a quite different magnetic configuration to a flare situated under the centre of the CME span and one might expect the two to be quite different.

5. Conclusions from the preceding analysis

The following points can be concluded from the above analyses:

1. There is a very strong association between flare and CME-onsets. Some 11% of all the flares studied were associated with CME-onsets and 40% of the CMEs studied had associated flare activity. The latter result is 3 times the expected association due to random chance. The association is enhanced even further, to a factor of over 5, when both spatial and temporal associations are considered.

2. Although there may be significant sensitivity effects which we cannot take into account here, as well as problems in defining and identifying flares and CMEs, for the present we must state that many flares do not have an association with an observed CME.

3. CME onsets are associated with flares of any duration. Some 6.4%, 25% and 50% of all flares of durations ~ 1 hr, ~ 3 hr and ~ 6 hr, respectively, are associated with CME-onsets. Thus, the longer the duration of the flare, the greater the chance that it is related to a CME. However, 60% of CME-associated flares have durations of under 2 hours; there is no evidence for a unique class of long duration flare event which is associated with CMEs.

4. The peak intensities for CME-related flares can be of any value, but tend to be greater (on average a factor of between 2 and 3 larger) than for the average flare. Whereas the distribution of flare intensities peaks at about the C1 level, for the CME-related flares, the peak shifts toward the M1 level.

5. The CME-related flares show significantly enhanced ratios of fall-times to rise times when compared to the full-flare data-set, i.e. the profile of a CME-related flare is, on average, less symmetrical than for the average flare. However, a CME-related flare can have any fall- and rise-time value.

6. In our temporal study, for the B, C and M-class flare events, the number of events associated with a CME are factors of 2.0, 4.4 and 6.9 greater than that expected from a random situation. This translates to a 6.8%, 15.1% and 23.7% chance of a CME observation in association with the observation of a B, C and M-class flare event, respectively. The association of CMEs, particularly with C and M-class events is striking.

7. The data support the view that the CME and flare onset are closely associated but that they can occur at anytime within several tens of minutes of one another, and that the CME onset altitude lies in the range 0 to $0.5 R_{\odot}$.

8. The site of a CME-associated flare tends to lie within the CME-span but may lie anywhere in the vicinity of the CME-span. There is no relationship between the site with respect to the CME-span and the nature of the flare, in terms of intensity and duration.

9. Finally, the above conclusions strongly support the view that the flare does not drive the CME-onset and vice versa.

6. The long duration event

We now discuss the so-called Long Duration Event and compare previously published studies on these events with the results of the current study.

The so-called long duration or decay event (LDE) has been linked to eruptive activity on the Sun for many years. However there has never been a universally accepted definition of such a class of event and there has never been a demonstration that such a unique class of event actually exists. Thus the studies of LDEs in association with CMEs are, at best, misleading. To understand the problem fully, we trace the history of the LDE.

Some years ago, Kreplin et al. (1962) detected an X-ray event of duration 6 hours which occurred at about the time of an eruptive prominence on the solar limb. The X-ray observation was made from an integrated-Sun device. Thus, no positional information is known about the X-ray emission. The X-ray event may well have been associated with the eruption, but it could not be confirmed.

Some 13 years later, Sheeley et al. (1975) published an examination of the soft X-ray profiles of the Skylab mission (1973/4). Using the full-Sun Solrad 9 1–8 Å data, they examined 19 events of duration over 4.5 hours, the arbitrary duration limit set to extract events of the type seen by Kreplin et al. Of the 19 events, 16 were detected during the operation period of the High Altitude Observatory's coronagraph on Skylab. Of those 16, 7 were co-incident in time with reported prominence eruptions, 7 were co-incident in time with CME activity (there were other possible associations) and as many were associated in time with $H\alpha$ flares.

Kahler (1977) examined the Solrad 9 1–8 Å X-ray data for the Skylab era. He chose to examine events for which the e-folding time was 0.87 hours or greater (a factor of 10 decrease in 2 hours or more). Again, a totally arbitrary definition was being used for event selection, designed to extract the longer duration X-ray events. Although the Solrad data were integrated-Sun, by simultaneously examining Skylab X-ray data and $H\alpha$ data,

Kahler concluded that these long lived events were associated preferentially with old active regions, and were arcade structures similar to those observed in the Skylab SO54 X-ray images and reported by Webb et al. (1976). These long duration events were shown to be related to prominence eruptions and CMEs.

Pallavicini et al. (1977) also addressed the LDE question. They used Solrad 9 data to identify any flare-like brightenings in X-rays during the Skylab period. Having linked the Solrad 9 events to $H\alpha$ and Skylab SO54 brightenings in order to study locations and sizes, they extracted the limb events, of which they had 43. A plot of duration versus altitude-achieved for these 43 events was used as a basis for defining two distinct types of X-ray event. Most events were clustered in the 4–100 minute duration interval, with altitudes of about 10^4 km. Six events appeared in an apparently distinct group with durations of 200–500 minutes and altitudes of 3–10 10^4 km. Pallavicini et al. associated all six events with CMEs seen by the High Altitude Observatory coronagraph on Skylab. Only 2 of the remaining, shorter duration events were associated with CMEs. No error bars were shown on the altitude versus duration plot. Since no accurate determination of the location of an event could be made to within say, at best, $\pm 5^\circ$ of the limb, this would introduce an error of several thousand km in the altitude estimate.

Sheeley et al. (1983) studied the association between CMEs and X-ray events for the 1979–81 period, using the Naval Research Laboratory's Solwind coronagraph aboard P-78-1 and the GOES 1–8 Å flux. Although no positional information was available for the X-ray data, based on relative timing alone, Sheeley et al. found a monotonic increase of the probability of CME association with X-ray event duration. Also, they showed that the X-ray durations (they did not consider durations of less than 30 minutes) displayed a continuous distribution, peaking at about 4 hours. Such a continuous distribution is not consistent with the interpretation that there are distinct classes of X-ray event. In other words Sheeley et al. indicated that an X-ray event could be associated with a CME, but that the longer the duration, the better the chance of the association, and that there is no distinct class of LDE, merely the tail of a single-event type X-ray distribution.

More recently, Webb & Hundhausen (1987) performed a statistical study of events associated with CMEs seen by the High Altitude Observatory's coronagraph on the Solar Maximum Mission, for the 1980 period of operation. They addressed also the question of the LDE. They defined an LDE as being an X-ray event with an e-folding decay time of over 12 minutes and demonstrating a good association with CME activity. However, the average X-ray peak intensity, the average CME speed and the average CME latitude were shown to be similar for both the short duration and LDE events of their data-set. No justification was given for the LDE definition.

Kahler et al. (1989) considered, also, the relationship between X-ray flare duration and CME-onset association. Whilst they did not set a minimum duration limit, they chose to examine only X-ray flares of intensity greater than M1. For these bright flares they showed that a CME could be associated with a flare of any duration.

Finally, St.Cyr & Webb (1991) studied active solar features in association with the CME observations made between 1984 and 1986. They showed that 34% of their CME-onsets were associated with X-ray flares (their Table III). This compares to our finding of 40% of the CME-onset windows containing X-ray flares. Whilst the majority of their report is well balanced and thorough (though they do not state how the X-ray flares were identified and selected, how their onset times and intensities were recorded), they do resort to a brief LDE analysis, using the same definition as Webb & Hundhausen (1987) and conclude that “most of the X-ray events that were associated with mass ejections were LDEs”.

The studies mentioned above are just a few of the studies involving LDEs, yet they can be considered to be representative. Let us summarise the principal problems of these LDE analyses: (i) They are based on several arbitrary and different definitions of LDE. (ii) Most rely on the association of CME and prominence activity with integrated-Sun X-ray data. This has inherent problems in locating the X-ray site and in the overlapping of remote X-ray enhancements. (iii) Most of the studies are influenced by earlier discussion of LDEs to the extent that filters are introduced to exclude the more frequent shorter duration flares. For example, Sheeley et al. (1975) introduced a filter which would have thrown away 96% of the flares in our study above, and would have excluded 76% of the flares which we find to be CME-associated. This filter had no physical basis.

Similarly, Sheeley et al. (1983) used a filter which would have excluded 28% of the X-ray events in our study and 19% of those events which we associated with CME onsets. Also, Kahler et al. (1989) chose to examine flares of intensity M1 and above. This represents only 5% of our flare data-set and would rule out 86% of the flares which the present study showed to be associated with CME-onsets. Again, these selections had no physical basis. The author believes that we cannot understand the physics of mass ejection or flare activity by masking significant portions of the data? Filters of this kind cannot be justified.

Let us consider a few more specific points from the studies discussed. Pallavicini et al. (1977) showed weak evidence to suggest different classes of X-ray burst, based on duration and size. Why is it that statistical studies of X-ray flare parameters have never revealed such classes? Studies by Culhane & Phillips (1970), Drake (1971), Sheeley et al. (1975) and Pearce & Harrison (1988), as well as the present work, show distributions of flare durations. None show any evidence to support the view that there are different flare classes dependent on duration. Sheeley et al. (1975) selected LDEs which subsequently showed an equal association with $H\alpha$ flares, CMEs and prominence eruptions, yet no-one is seriously stating that all $H\alpha$ flares must be accompanied by LDEs! *The logic is the same.*

The LDE discussion has caused great confusion and it is hoped that the present study can serve to put things into a better perspective. Clearly there is a lesson to be learned in that we must not blindly build in assumptions about classes of activity and artificially justify their existence by the use of biased analyses. Having said that, many of the findings of the present study are consistent with results from some of the LDE studies

mentioned, yet the analysis is clearly less biased. Let us drop the LDE terminology and talk about flare-related and non-flare-related CMEs without building in a bias toward a particular feature of the flare activity. Indeed, as mentioned above, 60% of all CME-related flares have durations of less than 2 hours.

7. Discussion

What can we conclude from the present study and the discussion above? First, we must recognise the intimate relationship between the flare and the CME, and build models accordingly. Flare models must cater for the CME, and vice versa. The distributions of flare characteristics for CME-related events which have been presented in this paper must be considered when the range of possible consequences of a flare-CME model are discussed. For example, such a model must be able to locate flare activity anywhere under the CME-span, must be able to cater for a flare of any duration and intensity, and must be able to cater for non-coincident flare and CME onset times. These sorts of complexities and asymmetries are rarely discussed by the modellers. It is the author's opinion, that the results are consistent with the view that the flare and CME are both symptoms of the same magnetic “disease”. That is, they are both driven by the same magnetic activity, e.g. shear or reconnection within the magnetic structure, and that they simply reflect the responses in different magnetic environments within the structure. In this way, they clearly do not drive one another, and their characteristics will be dependent on their own magnetic features rather than on one another, i.e. there is no basis for suggesting that a fast CME is more likely to be seen in association with a bright flare. A suggested approach, including a basic model which may cater for the requirements discussed above, has been presented by Harrison (1991). It involves the evolution of an asymmetrical hierarchy of magnetic loops which are consistent with active region loops, inter-active regions loops and flare loops, responding initially to shear in the active region.

In this final portion of the current paper, the aspect of the flare-CME relationship which we would like to concentrate on is that of event prediction. Most detected CMEs are near to the plane of the sky. Thus, they have little effect on the heliosphere in the vicinity of the Earth. However, a CME represents a very significant ejection of matter – up to 10^{13} kg of matter can be dumped into the solar wind, travelling at speeds of up to 2000 km s^{-1} . This results in a huge magnetic “disturbance” passing through the solar system and it is most likely the interaction of such a feature with the Earth's magnetosphere that drives much geomagnetic activity. Of course, the degree of the geomagnetic effect will depend on a number of things such as the magnetic field direction, the density and speed. However, it is of interest to predict the arrival of CMEs at the Earth. If we cannot view CMEs in the corona, which are directed at the Earth, then we must infer their onsets using proxy data. Therefore, given the CME-X-ray flare relationships given above, it is suggested that flare data can be used to predict geomagnetic activity, even though it is not directly related to such activity.

In the present study, we identified 151 CME events. When attempting to associate CME-onsets with flare-onsets and locations, we found 25 flares within our CME-onset windows as defined above. Since we may expect, maybe, 50% of the “surface” associations of CMEs to be behind the limb, this suggests that there was a flare in association with 33% of CMEs. Thus, if we can define a region on the Sun where CME eruptions are likely to interact with the Earth, for example, within 20° longitude and latitude of central meridian, we may infer that 33% of the flares which occur within that region will be associated with a CME which is likely to interact with the Earth’s magnetosphere.

So, how do we decide which 33% are the best CME candidates? Well, we have shown that about 7%, 15% and 24% of B, C and M class X-ray flares are associated with observed CMEs. We stress that this means some 86% of the CMEs will be associated with C-class flares or less – this fact alone demonstrates a significant departure from current geomagnetic prediction techniques through monitoring flare activity. Also, we have shown that longer duration events show a greater chance of CME association – for example, 6%, 25% and 50% for durations of about 1, 3 and 6 hours, respectively. Finally, we showed that flares with more asymmetrical profiles had a greater chance of CME association. Thus, to refine our geomagnetic prediction capabilities, it is suggested that a concerted effort be made to construct an algorithm which caters for all of these probabilities for a portion of the Sun’s disc where eruptions are likely to interact with the Earth.

References

- Burkepile J.T., St. Cyr O.C., 1993, A revised and expanded catalogue of mass ejections observed by the Solar Maximum Mission Coronagraph, NCAR Technical Note 369, January, 1993, Boulder, USA
- Culhane J.L., Phillips K.J.H., 1970, *Solar Phys.* 11, 117
- Drake J.F., 1971, *Solar Phys.* 16, 152
- Dryer M., 1994, *Sp. Sci. Rev.* 67, 363
- Fisher R.R., Munro R.H., 1984, *ApJ* 280, 428
- Harrison R.A., 1986, *A&A* 162, 283
- Harrison R.A., 1991, *Phil. trans. Roy. Soc. London A*, 336, 401
- Harrison R.A., Sime D.G., 1989, *A&A* 208, 274
- Harrison R.A., Sime D.G., 1992, in: *Proc. 26th ESLAB Symposium “Study of the Solar-Terrestrial System”*, ESA SP-346, p. 289
- Harrison R.A., Waggett P.W., Bentley R.D., et al., 1985, *Solar Pys.* 97, 387
- Harrison R.A., Hildner E., Hundhausen A.J., Sime D.G., Simnett G.M., 1990, *J. Geophys. Res.* 95, 917
- Hundhausen A.J., 1988, in: Pizzo V.J., Holzer T.E., Sime D.G. (eds.) *Proc. 6th Int. Solar Wind Conf.*, p. 181
- Hundhausen A.J., 1993a, in: Strong K.T., Saba J., Haisch B. (eds.) *The Many Faces of the Sun*
- Hundhausen A.J., 1993b, *J. Geophys. Res.* 98, 13177
- Kahler S.W., 1977, *ApJ* 214, 891
- Kahler S.W., 1992, *ARA&A* 30, 113
- Kahler S.W., Krieger A.S., Vaiana G.S., 1975, *ApJ* 199, L57
- Kahler S.W., Sheeley N.R., Liggett M., 1989, *ApJ* 344, 1026
- Kreplin R.W., Chubb T.A., Friedman H., 1962, *J. Geophys. Res.* 67, 2231
- Munro R.H., Gosling J.T., Hildner E., et al., 1979, *Solar Phys.* 61, 201
- Pallavicini R., Serio S., Vaiana G.S., 1977, *ApJ* 216, 108
- Pearce G., Harrison R.A., 1988, *A&A* 206, 121
- Sheeley N.R., Bohlin J.D., Brueckner G.E., et al., 1983, *ApJ* 272, 349
- Simnett G.M., Harrison R.A., 1985, *Solar Phys.* 99, 291
- Speich D.M., Tandberg-Hanssen, Wilson R.M., et al., 1975, *Solar Phys.* 45, 377
- St Cyr O.C., Webb D.F., 1991, *Solar Phys.* 136, 379
- Webb D.F., Krieger A.S., Rust D.M., 1976, *Solar Phys.* 48, 159
- Webb D.F., Hundhausen A.J., 1987, *Solar Phys.* 108, 383